# Impedance Analysis of a Power Line Distribution Network Using Short-Time Fourier Transform

Timothy O. Sanya*, Thokozani Shongwe‡, A. J. Han Vinck† *, and H.C. Ferreira*

*Deptartment of Electrical and Electronic Engineering Science, University of Johannesburg,
P.O. Box 524, Auckland Park, 2006, South Africa
tosanya@uj.ac.za, hcferreira@uj.ac.za

‡Deptartment of Electrical and Electronic Engineering Technology, University of Johannesburg,
P.O. Box 17011, Doornfontein, 2028, South Africa
tshongwe@uj.ac.za

†Institute of Digital and Signal Processing, University of Duisburg-Essen,
Bismarckstrasse 81, Essen, Germany
han.vinck@uni-due.de

***Abstract*—The impedance of a low voltage distribution network is analyzed and presented. Data collected from field measurement which was done over one week is used in this analysis. Basically, a chirp is injected into the electric grid, and the voltage and current signals (corrupted by various noises, including the 50 Hz mains signal) are time-sampled and stored for processing. The voltage and current are processed to obtain the impedance of the electric grid. Simulations are performed to establish the efficacy of the method of analysis used to obtain the impedance. The sliding window method of the Discrete Fourier Transform (DFT) is used in analyzing these impedance values. An eventual channel model describing the network is also presented.**

***Index Terms*—DFT, STFT, Impedance, Power Line Communications.**

## I. Introduction

The low impedance characteristic of a power line has been highlighted as one of the major factors militating against a significant commercial roll-off of the power line communications system. Some references on this topic can be found in [1]–[13], all of which have highlighted the low value of the power line access impedance. In [6], the characteristic impedance of a power line in the frequency range of 20–100 kHz is reported to be in the range of 0–80 Ω. The access impedance of the same channel is reported to be very low (0.5 mΩ–10 Ω) in [8]. The time and frequency dependent nature of the power line impedance is also its peculiar characteristic [1]. Perhaps [11] and [12] are the most recent works on this topic, in which the authors presented the access impedance characteristics of buildings up to 500 kHz using the voltage and current method as described in [10]. As pointed out in [5], these impedance measurements were taken under different power line environments and consequently have wide variation in value. In [1], [3], and [5], the inductive or capacitive characteristic of the power line channel has been established. The knowledge of the impedance of a network is essential for a successful point-to-point transmission between a transmitter and a receiver on the power line grid [3]. More measurements in determining the impedance characteristics of the network is essential as the network condition varies with time [10].

Since the condition of the network is hard to control, a possible solution to ensuring a reliable communication would be to adapt to the system. The aim of this work is to give information about the access impedance of a power line network. The impedance information can therefore enhance strategic positioning of modems in the network. The use of an impedance analyzer or a network analyzer would first come to mind for impedance measurement. However, these devices are useless when the data being analysed has already been collected and stored. As stated in [4], one can simply measure the output voltage and input current of a system, and divide them in the frequency domain to obtain the impedance characteristic of the system. To do this we employ the well known Discrete Fourier Transform (DFT) analysis which is a useful tool for frequency domain analysis.

The DFT takes discrete samples of signals, usually in the time domain, say $s(n)$, and translate them into their frequency components, say $S(k)$ as follows:

$$S(k) \;=\; \sum_{n=0}^{N-1} s(n) e^{\frac{-j2\pi kn}{N}}. \qquad (1)$$

Computationally, the DFT requires a longer time to compute, therefore the Fast Fourier Transform algorithm was developed to compute the DFT. In principle, the FFT algorithm computers the DFT but at a much lesser time. In this paper, the use of the term 'DFT' implies the FFT algorithm. This method, however, has a major downside, time and frequency resolution still

remains a major issue as far as this method is concerned. This problem is somehow explained by the Heisenberg uncertainty principle, which describes why time and frequency resolution cannot be increased simultaneously [13]. While increasing resolution in time, the frequency resolution decreases. One method of tackling this problem is truncating a sampled signal and do a DFT on the truncated signal. This method is termed "Short Time Fourier Transform" (STFT), a repetition of this process till the whole signal has been processed is termed "sliding window STFT".

The STFT is explained as follows: Let $f(n)$ be a time domain sampled sequence at sampling frequency $F_s$ over a period of time $T$, the total number of discrete samples $M$ is defined by $TF_s$. The $M$ samples of $f(n)$ can be grouped into $N = \frac{M}{a}$ samples, where each group of $N$ consecutive samples form a sequence $s(n)$ as follows:

$$s(n) = [f_{iN+1}, f_{iN+2}, \dots f_{(i+1)N}], \tag{2}$$

where $i = 0, 1, 2 \dots, a-1$, and $a$ is an integer that defines the length of $N$. A DFT is then performed on $s(n)$ for all the values of $i$ resulting in the STFT of $f(n)$.

This is the concept of the STFT, which is also known as the 'sliding window'. The short fall of this method is poor frequency resolution on the edges of the DFT output. One method of solving this problem is overlapping the DFT windows by a factor '$\alpha$', such that the relation in (2) becomes:

$$S(n, \alpha) = [f_{iN+1-\alpha}, f_{iN+2-\alpha}, \dots, f_{(i+1)N-\alpha}], \tag{3}$$

where $i = 1, 2, 3, \dots, a-1$.

The DFT window is defined by $s(n)$. There are other issues such as zero padding and data truncation depending on the choice of DFT window length, details of which are not mentioned here because they are well known attributes of the DFT method.

The motivation of this work was born out of the need to understand the impedance characteristics of a power line network. Also, to explain how the DFT can be used to analyze the impedance of an electrical network - thereby adding knowledge to the numerous existing results on the FFT algorithm, by giving a detailed step-by-step procedure in analyzing the impedance of a power line with the DFT method from a practical point of view. Also, in most cases, STFT analysis results are usually shown in spectrograms, in which the amplitude is shown as color intensity on a 2D frequency-time plot or as the height in a 3D frequency-time plot. This work shows how STFT is implemented while showing results on a 2D frequency-amplitude plane instead of the conventional way of showing STFT results.

## II. Simulations

In this section, the DFT sliding window method is investigated in the analysis of impedance. Two scenarios of the power line are assumed. A purely resistive system, and then a capacitive system are assumed. We would like to highlight at this point that these assumptions do not represent the power line channel model. The sole purpose is to test the efficacy of the DFT method we intend to apply to the actual field measurement.

### A. Resistive System Consideration

Consider the simple circuit in Fig. 1(a), with supply voltage, $V(t)$, and load of impedance, $Z$. Given that $V(t)$ is a cosine function with an amplitude $A$. A current $I(t)$ flows in the circuit according to the relation:

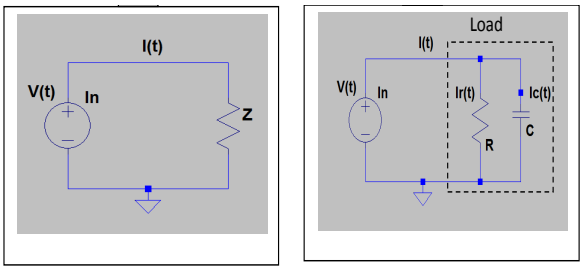


Fig. 1. (a). Purely Resistive System (b). Capacitive System.

$$u(t) = A\cos(2\pi f t). \tag{4}$$

Current $I(t)$ can be derived by dividing the relation in (4) by $Z$. $V(t)$ and $I(t)$ are sampled and transformed into their frequency domain components $V(f)$ and $I(f)$. The impedance $Z(f)$ of the system can therefore be retrieved according to (5)

$$Z(f) = \frac{V(f)}{I(f)}, \tag{5}$$

Since it is a resistive system, a constant impedance value for all frequency ranges should be expected. These values are compared with the known reference value of $Z$. If these values are equal, then the accuracy of this method is established.

Because of its frequency changing property, a linear chirp signal is used for this analysis as well as the field measurement. In Matlab, a chirp (0–250 kHz) voltage, sampled at 500 kHz with an amplitude of 2 $V_p$ is generated. An Impedance value of 2 $\Omega$ is assumed. The spectrogram of $V(t)$ is shown in Fig. 2.

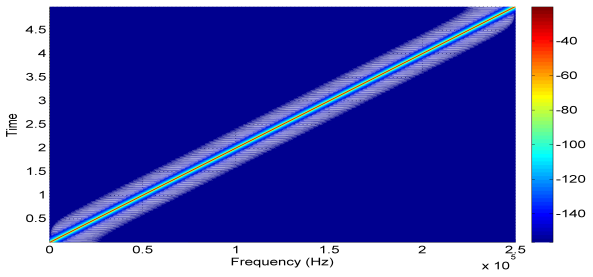


Fig. 2. Chirp signal for a noiseless system.

Applying STFT on $V(t)$ and $I(t)$ of the chirp signal for the circuit in Fig. 1(a), the image in Fig. 3 is obtained. At this stage no overlapping of samples is involved. This image depicts the plots of $V(f)$ and $I(f)$. The upper plot represents $V(f)$ while the lower plot represents $I(f)$. Attention should be given to the thin line that cuts across the dense region of each of the two plots, which after our careful observation is identified as the amplitude of the signal present. The lines are lines of best fit for the plots and they are achieved by applying a spline to the plots using the polynomial relation as described in [15].

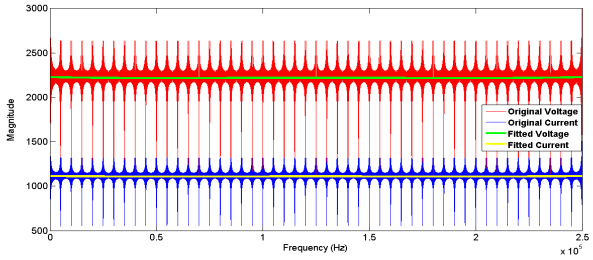


Fig. 3. $V(f)$ (V) and $I(f)$ (A) plots for a noiseless resistive system.

If Figure 3 is further zoomed in, spaces between different DFT windows can be observed. This is poor frequency resolution on the DFT edges and it is a consequence of applying the relation in (2). One way of combating this problem is by finding a line of best fit for the DFT magnitude. This solution is based on intuition which solely relies on the condition that the signal-to-noise ratio is significantly high, especially where background noise is concerned. $Z(f)$ is therefore derived according to the relation in (5). To achieve this, we implemented (5) in two different approaches:

- Direct division of $V(f)$ and $I(f)$, i.e.

$$\frac{|V(f)|}{|I(f)|} = \left( \frac{|a_1 + jb_1|}{|c_1 + jd_1|}, \frac{|a_2 + jb_2|}{|c_2 + jd_2|}, \ldots, \frac{|a_N + jb_N|}{|c_N + jd_N|} \right) \quad (6)$$

- Division using average values of $V(f)$ and $I(f)$ (line of best fit).

The essence of these two approaches is to find out how much effect the observed poor frequency resolution has on the eventual impedance value. The result of this investigation is shown in Fig. 4. It is evident that this method yields the 2 Ω impedance value for all frequencies as expected. Note that only one line is visible on the plot, this is because the two plots perfectly overlapped. The poor frequency resolution appears not to have any effect on the result, this is explained by the fact that the voltage and the derived current thereof are similar for a purely resistive load. One can therefore conclude that any error introduced into the voltage as a result of DFT

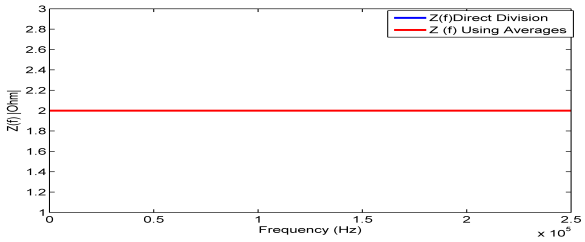


Fig. 4. Impedance $Z(f)$ derived with the DFT sliding window method (resistive noiseless channel).

would be the same for the current, hence the effect would be canceled out with division.

We consider a simulated channel with three types of known noise associated with the power line channel. The three types of noise added to the voltage signal are:

1) Narrow-band noise;
2) Impulse noise;
3) Background noise.

For more information about these types of noise, reader is referred to [18].

Fig. 5 is a spectrogram showing how these noises affect the chirp signal. The vertical lines represent narrow band noise; the horizontal lines represent impulse noise, while white Gaussian noise is used as background noise, it fills all the spectrum.

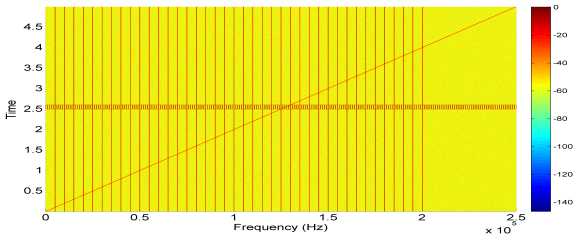


Fig. 5. Spectrogram of a chirp signal (voltage) for noisy system that is resistive.

A first glance at Fig. 5 immediately shows the effectiveness of the STFT method as far as a transient signal is concerned. Apart from the background noise that spreads over the spectrum, the other two types of noise only affect the chirp at a specific point. For example, the chirp is only affected by the the impulse noise around 125–130 kHz, 2.5s approx. The narrow band noise therefore poses more problem as it occurs more frequently. One solution is to avoid these noises in analysis and use interpolation to get the values for the affected frequencies - this, however, we find to be computationally difficult. Another solution would be to perform a STFT on the signal without avoiding the noise spectrum. An estimate of the actual value can be found by using the coefficients of the relation in (6). This second solution is applied in this work. The reader is referred to [16], [17], and any Matlab documentation on curve fitting and least squares approximation method. For the purpose of this analysis, these narrow-band noises are

spaced 5 kHz apart. The spacing is in agreement with the observed harmonics from the field measurement.

Fig. 6 demonstrates how noise affects the STFT method, where the direct division of $V(f)$ by $I(f)$ is found to yield error. However, the average values yielded the expected 2 Ω impedance value. As a result of this, only result from average values obtained from finding a line of best fit for the STFTs will be presented in the remaining sections of this work.

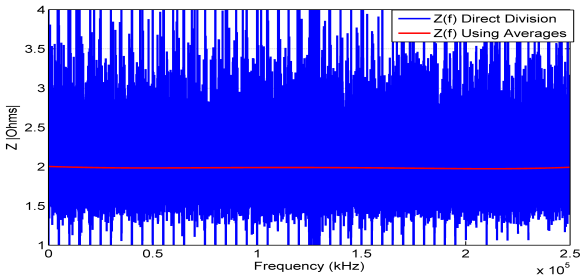


Fig. 6. Impedance $Z(f)$ derived with the DFT's sliding window method (resistive noisy channel).

### B. Capacitive System Consideration

For the second scenario of our DFT test, we consider a simple parallel network of a resistor and a capacitor (Fig. 1(b)). This type of circuit not only has a frequency dependent impedance characteristic, there is also a difference between the phases of the voltage and current in the circuit [15]. The aim is to test how these characteristics influence the STFT result.

Given a parallel RC circuit as shown in Fig. 1(b), we can compute the instantaneous impedance according to the relation:

$$Z(\omega) = \frac{R}{(1 + j\omega RC)}, \tag{7}$$

where, $R = 10\ \Omega$ and $C = 10^{-6}$ F; $\omega = 2\pi f$.

The instantaneous impedance values obtained from (7) will be compared with the DFT method which is applied to both $V(t)$ and $I(t)$. The total current can be determined by applying Kirchhoff's current law.

Using a chirp that spans between 20 kHz–80 kHz and sampled at 1 MHz, A STFT is obtained for the voltage and current signal. The limitation to this frequency range for the capacitive system is a deliberate action. In order to derive current from a given voltage, the signal has to be over-sampled. However, this is computationally uneconomical, we therefore restrict analysis to lower frequency region (up to 80 $kHz$).

Attention is called to Fig. 7. Here the plot shows impedance values from the STFT and the calculated impedance with the use of (7). The STFT can be seen to deviate from the calculated impedance as the frequency increases. This deviation is attributed to the method by which $I(t)$ was derived, which translates to the need for a very high sampling frequency as stated in the previous paragraph. The percentage deviation is therefore shown in Fig. 8. Although not shown here, the STFT method approaches the calculated values with an increase in the sampling frequency.

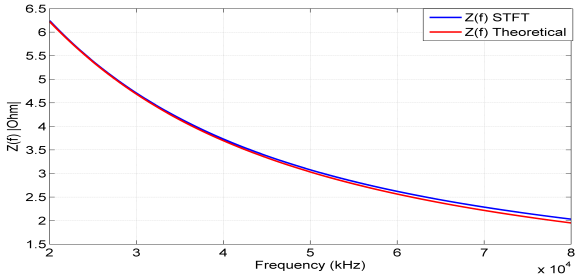


Fig. 7. Comparison of calculated impedance values with the STFT derived values for a noiseless capacitive system.

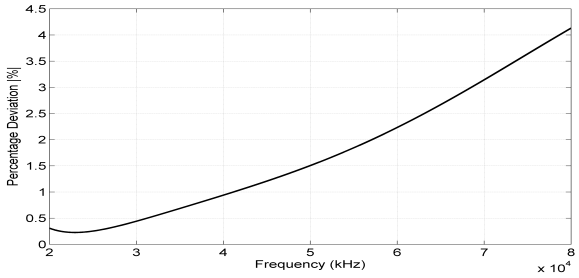


Fig. 8. Percentage deviation. *(The DFT method deviates from ideal due to insufficient sampling).*

The last test of the sliding window DFT is the noisy scenario of the capacitive system. The same noise scenario as the resistive system is applied. The same types of noise are added to the voltage and current signals. The resulting impedance (Fig. 9) indicates error caused by these noises. However we find these errors to be in an acceptable limit.

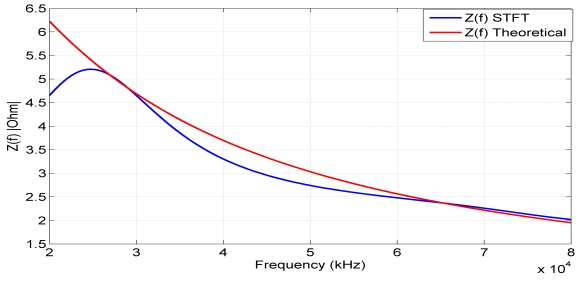


Fig. 9. Comparison of calculated impedance values with the STFT derived values for a noisy capacitive system.

## III. Applying the Sliding Window to Field Measurement

This section covers the implementation of the method described in the previous section on an actual field measurement.

This measurement was done in an area called Kastel in the Netherlands. Fig. 10 shows the measurement setup, while Fig. 11 shows a summary of the impedance analysis process. The data is captured and stored using a program called Dewesoft. The stored information is further processed and analyzed in Matlab. Since the data contains low frequency components such as the 50 Hz mains signal, filtering becomes necessary. This high pass filter in Fig. 11 filters the low frequency components present in the data. Also it is necessary to note that the low pass filter in Fig. 11 is only serving the purpose of windowing, a Kaiser window is used in this case. From Fig. 10, the tick line between the transformer and the feeder branch represents the three phases (red, blue, and green) of the power line network. A chirp signal is injected into one of the phases at any point in time. The voltage and current flowing in the lines are measured and stored at 500 kHz sampling frequency. As stated in [6], it is worth mentioning that crosstalk across the phases is observed, this, however, is beyond the scope of this work.

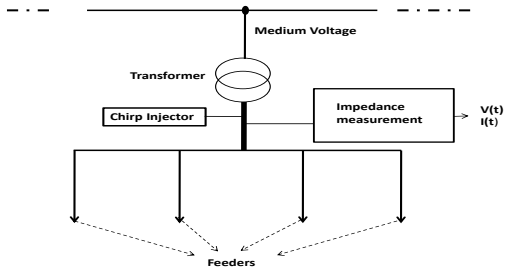


Fig. 10. Field measurement setup.

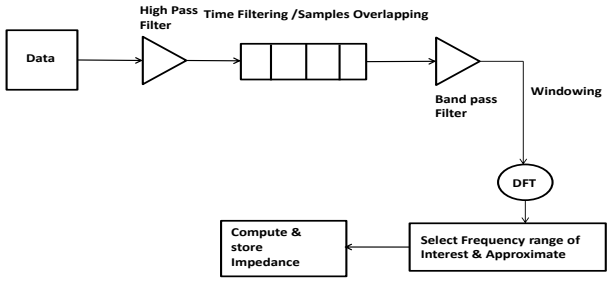


Fig. 11. Summary of impedance analysis process.

A very first observation from the spectrogram plot of the data are the harmonics spaced at approximate value of 5 kHz apart. Their source is traced to some variable frequency drives (VFDs) present in the transformer station. These harmonics are identical to the vertical lines shown in Figure 5. It is also observed the their signal strength fades away in the higher frequency region.

After applying the sliding window DFT to the data, the first observation is that the curve fitting approximation method failed dismally in comparison to the result obtained in the simulations section. This problem is solved by curve fitting individual DFT window before bringing them together. A comparison between Fig. 3 and Fig. 12 shows a clear improvement in the approximation method. It therefore goes without saying that overlapping the DFT windows improves the poor frequency resolution on the edges.

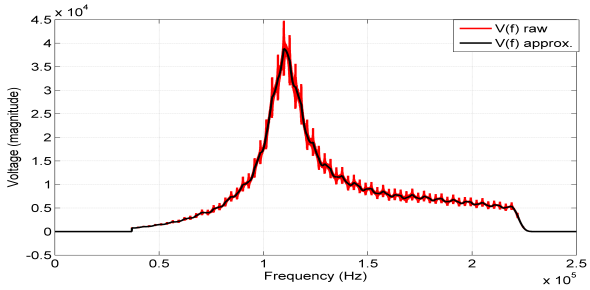


Fig. 12. $V(f)$ of a chirp from field measurement showing improvement in approximation method.

Finally, the estimated impedance values of loaded phases of a medium voltage transformer are shown in Fig. 13. The word 'estimate' is used to describe these values, because approximations have been used in arriving at the values. Fig. 13 shows a resonant behavior of the load, which suggests some reactive property of the connected load. The dynamic nature of the power line impedance is further established here. The lower frequency region (30–50 kHz approx.) shows the effect of low SNR, values in this region are not reliable.

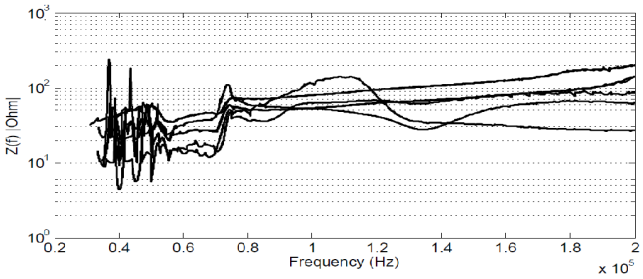


Fig. 13. Impedance of a power line load for different phases.

## IV. Modelling the Power Line Channel

This section gives a simple model of circuit elements that can be connected to obtain results approaching (or comparable to) those obtained from the real data of the power line network.

Fig. 14 is a diagram of the secondary side of a loaded 3-phase transformer, with a voltage signal $V$ injected into one of the phases. This shows more information about the measurement setup as well as explains the cross-talk observed across phases. A simplified network model of Figure 14 is shown in Fig. 15. Each phase is represented by an inductor, with the inductance represented by $P_1$, $P_2$, $P_3$ for phase-1, phase-2, and phase-3 respectively. Assuming all series parameters are negligible for the purpose of analysis, the load on each phase can be represented by a parallel $LC$ circuit with a resistor connected in series with the inductor.

The impedance, $Z_{\text{P1}}$, of $coil_1$ is given by:

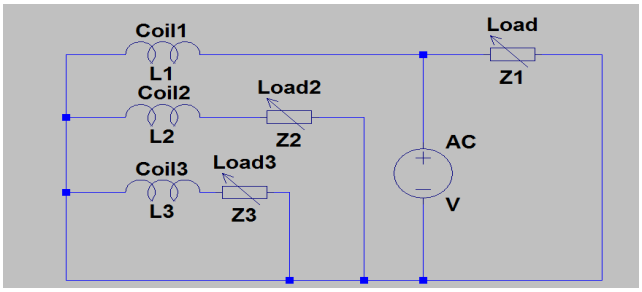


Fig. 14. Loaded 3-Phase transformer circuit.

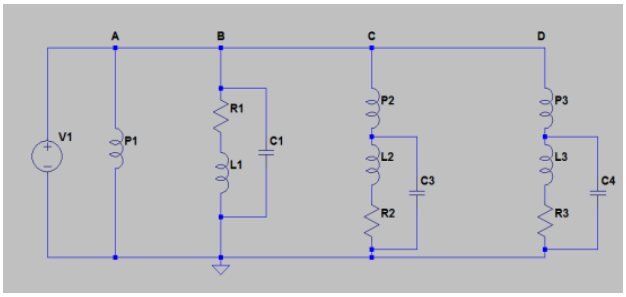


Fig. 15. Simplified power line channel model.

$$Z_{\mathrm{P1}} = j\omega P_1. \tag{8}$$

If the coils have equal impedance values, then, $Z_{\mathrm{P1}} = Z_{\mathrm{P2}} = Z_{\mathrm{P3}}$.

From (8), it is evident that the impedance value approaches infinity as the frequency increases. Also, assuming $Z_1 = Z_2 = Z_3$, then branch $B$ will sink almost all the current flowing in the circuit. Branches $A$, $C$, and $D$ can be replaced with an open circuit. Therefore the observed cross-talk across phases from the field measurement can only be coupled through air and not through the transformer. In our simulations, the behavior of the load in branch $A$ is comparable to those shown in Fig. 13. The resonant characteristic of the load depends on the value of the capacitor. Also, the resistance value determines the minimum value of the impedance.

## V. Conclusion

This work has presented the impedance characteristics of a power line network from a measurement point of view and simulations have been used to justify the results. STFT with Matlab is used in analyzing these measurements. In this work, results from actual field measurements have been presented. A step-by-step procedure on how STFT can be implemented from a practical point of view has also been presented. Absolute values have only been presented in this work. This is a bottleneck of the DFT method, in the presence of noise, signal reconstruction from the STFTs becomes very difficult. The impedance value ranges from 12 Ω to a maximum of 200 Ω in the frequency range of 50 kHz–200 kHz.

## Acknowledgment

The authors would like to thank Alliander® [1] company for sponsoring this work and for making the measurement data available. Special thanks to Mr. Kiwi Smit, also from the Alliander® company, for his inputs, most of which are elaborate in this work.

## References

[1] J.R. Nicholson and J. A. Malack, "RF Impedance of Power Lines and Line Impedance Stabilization Networks in Conducted Interference Measurements," in *IEEE Transactions on Electromagnetic Compatibility*, vol. EMC-15, no. 2, May. 1973, pp. 84–86.

[2] J. A. Malack and J. R. Engstrom, "RF Impedance of United States and European Power Lines," in *IEEE Transactions on Electromagnetic Compatibility*, vol. EMC-18, no. 1, Feb. 1976, pp. 36–38.

[3] R. M. Vines, H. J. Trussell, K. C. Shuey, and J. B. O'Neal Jr, "Impedance of the Residential Power-Distribution Circuit," in *IEEE Transactions on Electromagnetic Compatibility*, vol. EMC-27, no. 1, Feb. 1985, pp. 6–12.

[4] Adly A. Girgis and R. Brent McManis, "Frequency Domain Techniques for Modeling Distribution or Transmission Networks Using Capacitor Switching Induced Transients," in *IEEE Transactions on Power Delivery*, vol. 4, no. 3, Jul. 1989, pp. 1882–1890.

[5] J. B. O'Neal Jr, "The residential Power Circuit as a Communication Medium," in *IEEE Transactions on Consumer Electronics*, vol. CE-32, no. 3, Aug. 1986, pp. 567–577.

[6] H C. Ferreira, H. Grove, O. Hooijen, and A J. Han Vinck , "Power Line Communications: An Overview," in *Proc. IEEE AFRICON*, Cape–Town, South–Africa, Sep. 1996, pp. 558–563 .

[7] M. Arzberger, K. Dostert, T. Waldeck, and M. Zimmermann "Fundamental Properties of the Low Voltage Power Distribution Grid," in *Proc. Int. Symp. Power Line Commun. and its Appl.*, Essen, Germany, Apr. 2–4, 1997, pp. 45–50.

[8] Olaf, G. Hooijen, "A Channel Model for the Low-Voltage Power-Line Channel; Measurement - and Simulation Results," in *Proc. Int. Symp. Power Line Commun. and its Appl.*, Essen, Germany, Apr. 2–4, 1997, pp. 51–56.

[9] N. Pavlidou, A. J. H. Vinck, J. Yazdani, and B. Honary, "Power line communications: state of the art and future trends," in *IEEE Communicationss Magazine*, vol. 41, no. 4, Apr. 2003, pp. 34–40.

[10] M. Sigle, Liu Wenqing, and K. Dostert, "On the impedance of the low-voltage distribution grid at frequencies up to 500 kHz," in *Proc. Int. Symp. Power Line Commun. and its Appl.*, Beijing, China, Mar. 27–30, 2012, pp. 30–34.

[11] Guangbin Chu, Jianqi Li, and Weilin Liu, "Narrow Band Power Line Channel Characteristics for Low Voltage Access Network in China," in *Proc. Int. Symp. Power Line Commun. and its Appl.*, Johannesburg, South Africa, Mar. 24–27, 2013, pp. 297–302.

[12] H. Gassara, F. Rouissi, A. Ghazel, "On the Characterization of the Indoor Low-Voltage PLC Channel At Frequency Up to 500 kHz," in *Proc. Int. Symp. Power Line Commun. and its Appl.*, Johannesburg, South Africa, Mar. 24–27, 2013, pp. 303–308.

[13] P. J. Loughlin, J. W. Pitton, "Proper time-frequency energy distributions and Heisenberg uncertainty principle," in *Proc. IEEE-SP International Symposium on Time-Frequency and Time-Scale Analysis*, Victoria BC, USA, Oct. 4–6, 1992, pp. 151–154.

[14] The Mathworks, "Polynomial curve fitting" Online: http://www.mathworks.de/de/help/matlab/ref/polyfit.html, Sep. 2013

[15] H.W. Sorenson, "Least-squares estimation: Gauss to Kalman," in *IEEE Spectrum*, vol. 7, Issue. 7, Jul. 1970, pp. 63–68.

[16] Erich Fuchs, Thiemo Gruber, Jiri Nitschke, and Bernhard Sick, "Online Segmantation of Time Series Based on Polynomial Least-Squares Approximations," in *IEEE Transactions on Pattern Analysis and Machine Intelligence*, vol. 32, No. 12, Dec. 2010, pp. 2232–2245.

[17] Hendrik C. Ferreira, Lutz Lampe, John Newbury, Theo G. Swart, "Channel Characterization," in *Power Line Communications: Theory and Applications for Narrowband and Broadband Communications over Power Lines*, 1st ed., May. 2010, pp. 7–126.

[1] Alliander is a utility company in the Netherlands.